Structure and Stability of Molecular Crystals with Many Body Dispersion inclusive Density Functional Tight Binding

Majid Mortazavi,[†] Jan Gerit Brandenburg,[‡,¶,§] Reinhard J. Maurer,[*,‖] and Alexandre Tkatchenko[*,⊥,†]

†*Fritz-Haber-Institut der Max-Planck-Gesellschaft, Faradayweg 4-6, 14195 Berlin, Germany*

‡*Department of Chemistry, University College London, 20 Gordon Street, WC1H 0AJ London, UK*

¶*London Centre for Nanotechnology, University College London, 17-19 Gordon Street, WC1H 0AJ London, UK*

§*Thomas Young Centre, University College London, Gower Street, WC1E 6BT London, UK*

‖*Department of Chemistry and Centre for Scientific Computing, University of Warwick, Gibbet Hill Road, Coventry CV4 7AL, United Kingdom*

⊥*Physics and Materials Science Research Unit, University of Luxembourg*

E-mail: r.maurer@warwick.ac.uk; alexandre.tkatchenko@uni.lu

Computational Details

The X23 benchmark dataset represents a mixture of systems dominated by Hydrogen, vdW, and combined Hydrogen-vdW bonding interactions.[1,2] In the absence of high-level theoretical reference data due to enormously large computational cost and complexity, experimental

sublimation enthalpies are used for comparison. For a direct comparison between experimental sublimation enthalpies and theoretical lattice energies, vibrational contributions have been properly removed from the experimental sublimation enthalpies. Similarly an accurate description of geometries requires careful consideration of thermal contributions, however, we disregard this effect in both density functional tight-binding and density functional theory calculations. Herein, we aim to provide a relative overview of the recently implemented vdW-inclusive DFTB as compared to vdW-inclusive DFT methods.

Coumarin Details

For the polymorphic system under study, we choose to study coumarin ($C_9H_6O_2$)—a small rigid molecule with unusually rich polymorphism.[3] Coumarin has diverse applications ranging from cosmetics to medicine and agriculture, and there are currently five experimentally observed polymorphs. Its rich polymorphic effect, dominant intermolecular interactions, and extremely narrow energy differences of polymorphs (within a few kJ mol^{-1}) has made it a quite challenging problem from both the experimental and theoretical point of view. A number of vdW-inclusive DFT methods were used for stability ranking of coumarin polymorphs with very few returning correct ranking, which makes it a challenging test case for vdW-inclusive DFTB.

Damping Parameters

The optimized damping parameters are 1.05 (aka *s_r* parameter) for TS, 1.0 (aka *beta* parameter) for MBD. The damping function parameters of D3 for the DFTB3(3ob) were fitted only based on S66 energies, and are used as originally reported in Ref. 4. Table S3 gives a summary of the datasets used for the fitting procedure. Apart from the slightly different fitset, the functional form differs in all three correction schemes. D3 can be used with a one-parameter zero damping or a two-parameter rational damping function both directly acting on the energy contributions. TS uses a similar zero damping, while in MBD the damping

acts on the dipole interaction, which leads to differences in the fitting behaviours.

Table S1: The absolute value of X23 crystals volume (in Å^3) obtained using PBE/DFTB3+vdW optimization along with experimental volumes.

	Systems	Exp.	PBE+D3	PBE+TS	PBE+MBD	DFTB3+D3	DFTB3+TS	DFTB3+MBD
0	1,4-Cyclohexanedione	279.6	282.3	278.1	277.0	246.1	261.2	266.4
1	Adamantane	393.1	391.9	369.4	373.8	352.2	362.9	381.0
2	Anthracene	456.5	461.3	451.1	456.6	415.4	440.5	451.5
3	Benzene	474.1	465.1	463.8	464.3	411.2	446.5	448.8
4	CO2	177.9	185.3	195.1	190.6	155.1	169.1	167.2
5	Hexamine	329.9	333.3	334.8	330.2	316.2	327.7	345.3
6	Naphtalene	340.8	348.6	340.6	343.5	310.0	334.3	339.8
7	Pyrazine	203.6	197.6	195.8	201.5	180.6	196.4	206.9
8	Pyrazole	698.3	714.3	711.8	715.6	654.9	659.3	712.3
9	1,3,5-triazine	586.8	552.7	553.7	571.5	502.1	545.7	543.5
10	1,3,5-trioxane	616.5	619.2	608.0	612.5	558.5	581.6	584.6
11	Cytosine	472.4	471.9	461.7	475.4	429.6	462.2	478.2
12	Imidazole	348.8	365.4	341.9	349.7	316.4	343.7	352.2
13	Uracil	463.4	458.6	452.5	464.7	416.7	440.0	443.6
14	Acetic-Acid	297.3	301.9	294.1	298.8	260.0	276.8	278.9
15	Ammonia	135.1	124.3	123.1	125.8	93.2	102.3	98.2
16	Cyanamide	415.7	413.5	420.2	422.4	380.9	418.7	410.7
17	Ethylcarbamat	248.8	247.6	238.7	242.4	222.8	233.6	236.9
18	Formamide	224.1	222.9	221.5	226.7	199.6	218.6	218.5
19	alpha-Oxalic-acid	312.6	315.7	315.5	316.3	270.3	281.6	281.0
20	beta-Oxalic-acid	156.9	159.5	159.2	159.6	137.4	144.5	146.8
21	Succinic-Acid	243.9	248.0	244.0	245.4	213.1	228.2	229.9
22	Urea	145.1	144.0	145.5	144.2	136.4	142.1	141.3

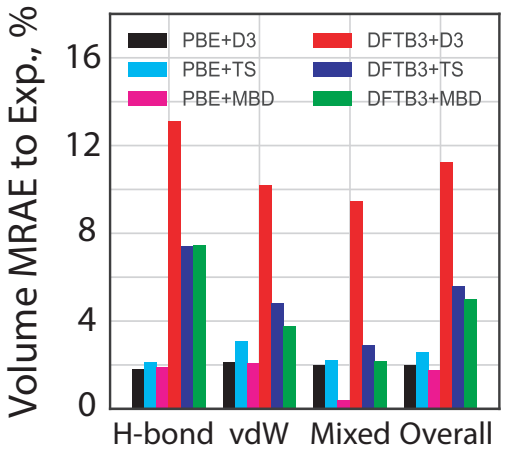

Figure S1: The X23 dataset geometry analysis using DFT(B)+vdW methods in terms of Mean of RMSD values as calculated with respect to experimental geometries

Table S2: X23 crystals lattice energies (in kJ mol^{-1}) obtained using PBE/DFTB3+vdW optimization along with experimental energies.

	Systems	Exp.	PBE+D3	PBE+TS	PBE+MBD	DFTB3+D3@ DFTB3+D3	PBE+D3@ DFTB3+D3	DFTB3+TS@ DFTB3+TS	PBE+TS@ DFTB3+TS	DFTB3+MBD@ DFTB3+MBD	PBE+MBD@ DFTB3+MBD
0	1,4-Cyclohexanedione	-88.6	-89.10	-106.50	-92.38	-105.64	-79.31	-89.76	-102.42	-75.42	-88.44
1	Adamantane	-69.4	-72.42	-109.97	-80.38	-97.09	-69.25	-89.28	-110.27	-61.34	-79.56
2	Anthracene	-112.7	-104.59	-135.96	-107.40	-130.93	-101.63	-101.65	-134.58	-74.94	-106.48
3	Benzene	-51.7	-55.56	-67.12	-54.72	-66.02	-51.59	-49.33	-66.80	-37.92	-54.55
4	CO2	-28.4	-23.49	-24.06	-23.58	-24.09	-20.24	-16.40	-23.09	-15.49	-21.74
5	Hexamine	-86.2	-86.27	-114.51	-89.91	-84.96	-84.60	-73.08	-114.22	-52.11	-91.20
6	Naphtalene	-81.7	-78.23	-101.11	-80.44	-97.78	-75.85	-74.48	-100.47	-55.25	-80.02
7	Pyrazine	-61.3	-66.26	-75.63	-62.81	-64.36	-63.34	-49.09	-74.81	-37.12	-61.65
8	Pyrazole	-77.7	-82.21	-88.96	-82.56	-62.26	-75.84	-62.30	-82.18	-42.07	-77.70
9	1,3,5-triazine	-61.7	-61.47	-69.14	-57.57	-59.26	-57.59	-43.46	-70.39	-33.41	-58.13
10	1,3,5-trioxane	-66.4	-59.42	-76.00	-64.05	-64.81	-57.59	-59.28	-76.81	-48.79	-66.47
11	Cytosine	-169.8	-162.17	-173.34	-162.04	-154.54	-145.84	-131.53	-162.25	-118.90	-153.98
12	Imidazole	-86.8	-92.78	-102.12	-93.82	-74.72	-86.47	-62.52	-99.09	-53.37	-90.03
13	Uracil	-135.7	-138.47	-148.95	-138.34	-149.19	-129.20	-126.12	-143.63	-117.74	-133.29
14	Acetic-Acid	-72.8	-75.02	-82.37	-76.95	-82.69	-67.52	-71.93	-80.45	-65.58	-74.45
15	Ammonia	-37.2	-43.33	-44.65	-43.02	-40.72	-33.28	-30.66	-41.15	-35.51	-36.99
16	Cyanamide	-79.7	-93.77	-94.38	-93.01	-67.95	-85.09	-54.24	-88.64	-51.75	-84.91
17	Ethylcarbamat	-86.3	-88.50	-99.75	-91.77	-99.47	-83.83	-87.74	-97.54	-78.23	-90.37
18	Formamide	-79.2	-82.85	-86.24	-82.76	-78.94	-78.82	-68.39	-85.63	-64.07	-81.72
19	alpha-Oxalic-acid	-96.3	-93.42	-100.29	-96.11	-123.62	-66.95	-106.12	-79.71	-101.71	-76.28
20	beta-Oxalic-acid	-96.1	-96.48	-103.51	-98.51	-128.55	-74.18	-110.82	-84.86	-106.38	-82.98
21	Succinic-Acid	-130.3	-133.40	-148.79	-137.75	-151.50	-116.94	-130.65	-140.49	-118.83	-131.03
22	Urea	-102.5	-109.00	-112.24	-110.14	-112.16	-107.13	-98.42	-112.08	-94.43	-109.96

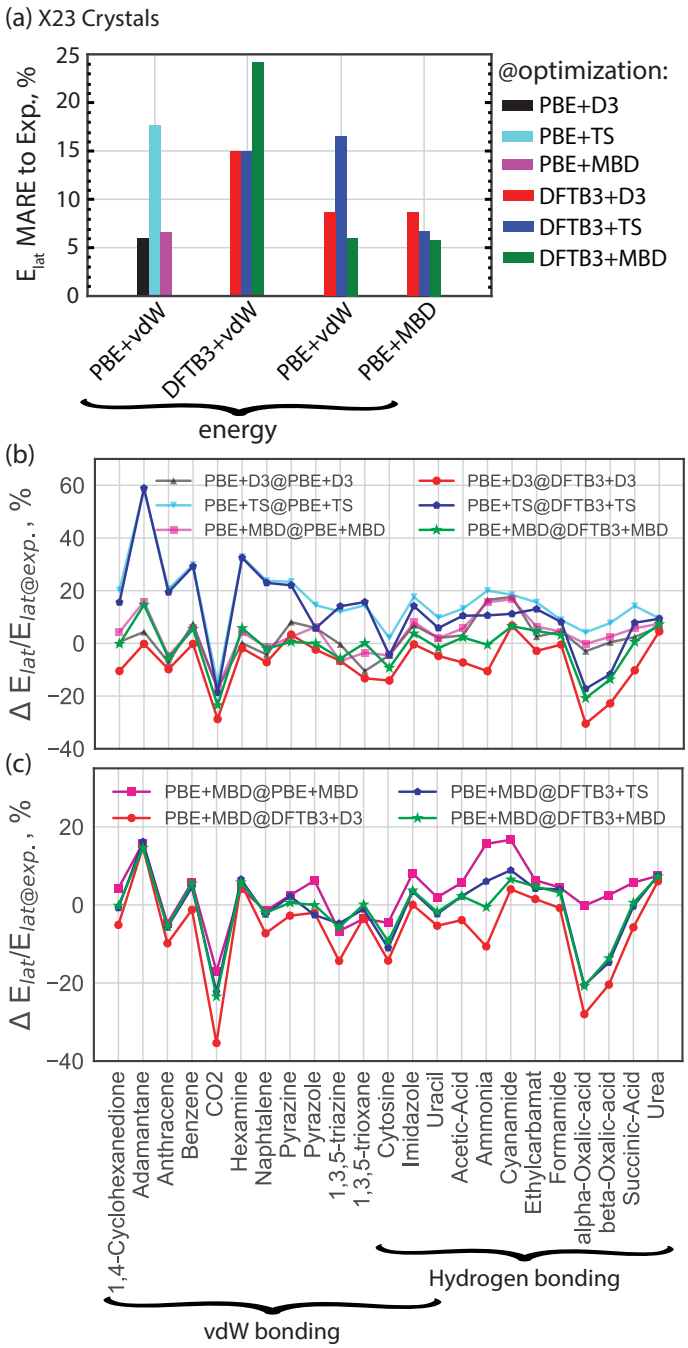

Figure S2: The X23 dataset lattice energies analysis using DFT(B)+vdW methods in terms of: (a) Mean absolute relative errors (in %) of the lattice energies, and (b) Relative error (in %) of lattice energies following PBE+vdW@PBE+vdW/DFTB3+vdW abbreviation, (c) Relative error (in %) of lattice energies following PBE+MBD@DFTB3+vdW together with PBE+MBD@PBE+MBD results, all with respect to the experimental values. The following abbreviation use isd in all legends: 'level of theory for energy evaluation'@'level of theory for geometry optimization'. For example in subfigure (a) for PBE+vdW geometries, energy evaluation is carried out at corresponding PBE+vdW level (first column). Whereas for DFTB3+vdW, energy evaluation is done three levels: corresponding DFTB3+vdW (second column), corresponding PBE+vdW level (third column), PBE+MBD level (fourth column).

Table S3: The datasets used for fitting dispersion parameters.

Dispersion	D3	TS	MBD
Electronic			
DFT(PBE)	S22	S22	S66x8
DFTB(3ob)	S66	S66x8	S66x8

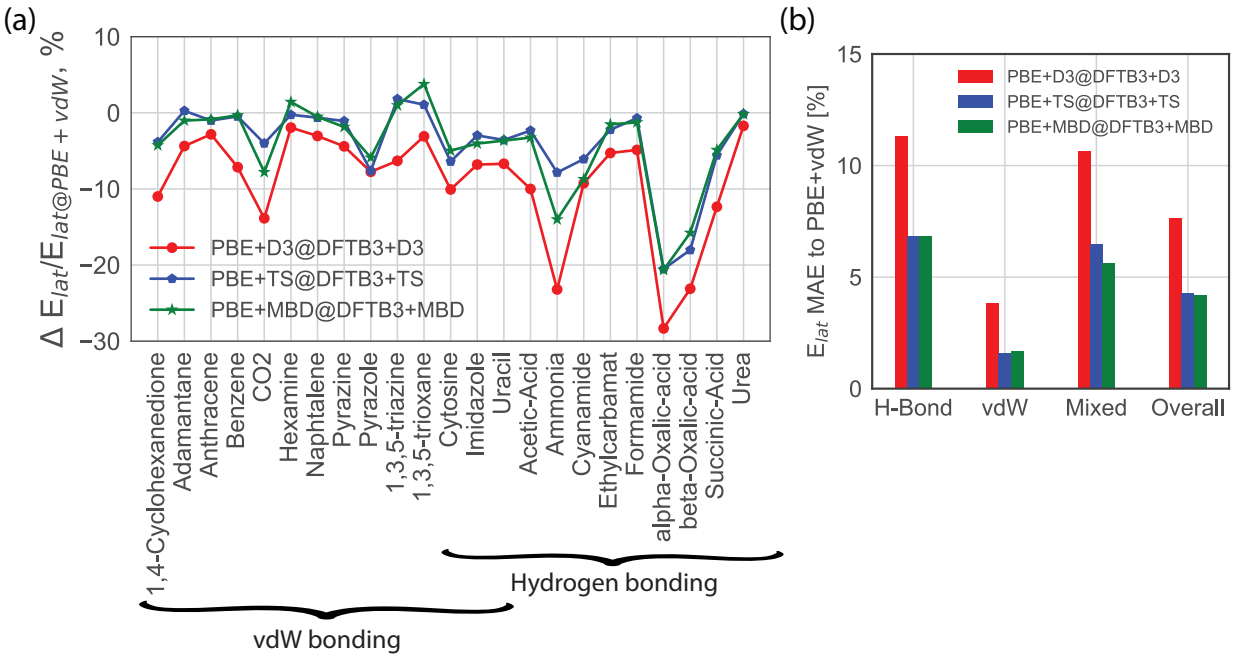

Figure S3: The X23 dataset lattice energies analysis using DFTB3+vdW methods in terms of: (a) Mean absolute relative errors (in %) of the lattice energies, and (b) Relative error (in %) of lattice energies, both with respect to PBE+vdW energies.

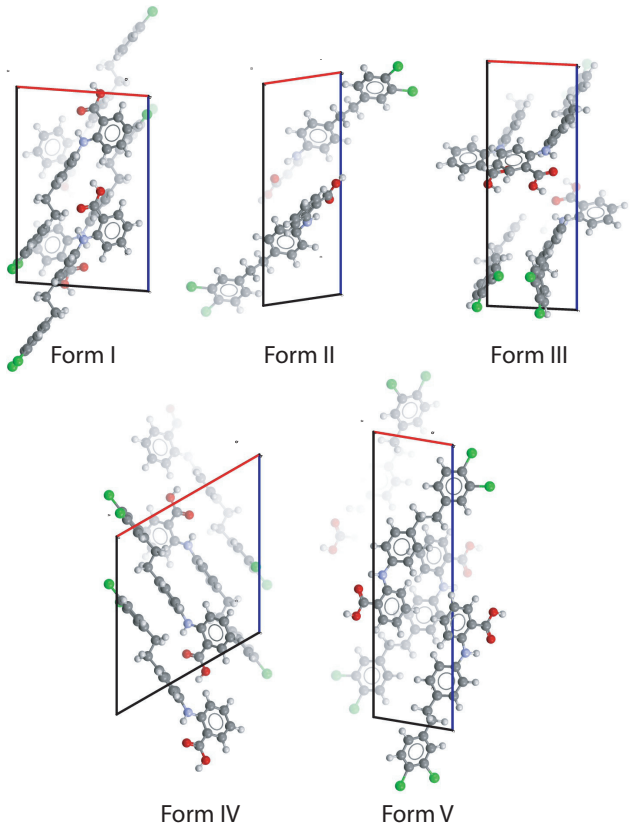

Figure S4: Molecular models of the five most stable experimentally observed XXIII polymorphs

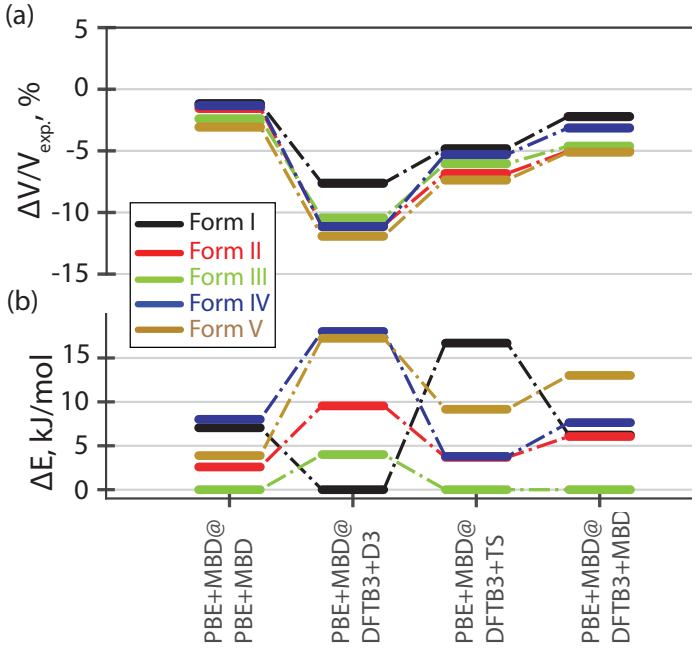

Figure S5: Comparison of DFT(B)+vdW methods for XXIII polymorphs in terms of: (a) optimized unit cell volumes $\Delta V/V_{exp}$ in% w.r.t. experimental structures (determined at 257 or 293 K), (d) stability rankings based on lattice energies ΔE in kJ mol^{-1}.

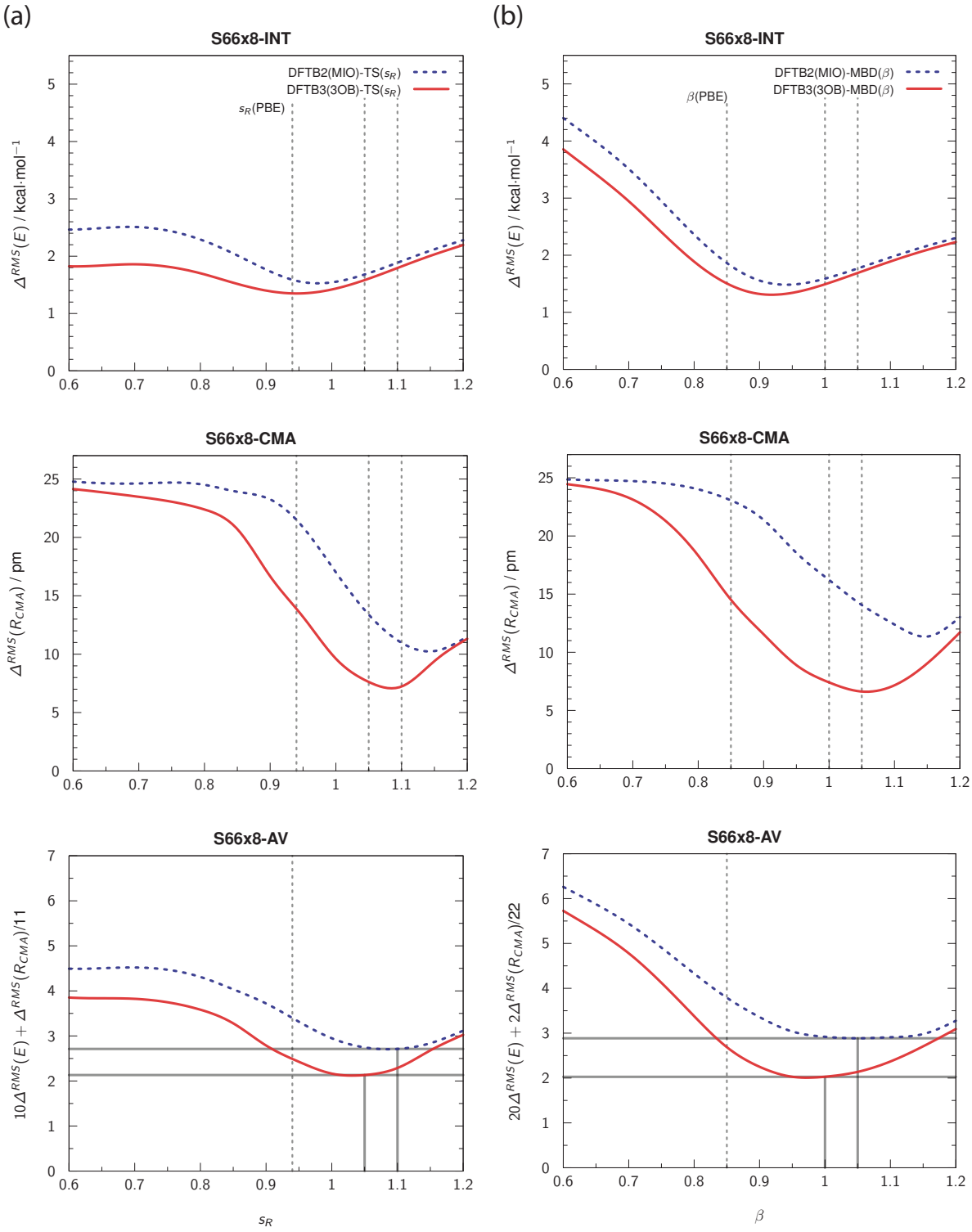

Figure S6: The fitting procedure of (a) TS, (b) MBD damping parameters for the DFTB3(3OB, MIO) done on the s66x8 set[5,6] using both energy and geometry information of the splined minimum.

References

(1) Otero-De-La-Roza, A.; Johnson, E. R. *J. Chem. Phys.* **2012**, *137*, 054103.

(2) Reilly, A. M.; Tkatchenko, A. *J. Chem. Phys.* **2013**, *139*, 024705.

(3) Shtukenberg, A. G.; Zhu, Q.; Carter, D. J.; Vogt, L.; Hoja, J.; Schneider, E.; Song, H.; Pokroy, B.; Polishchuk, I.; Tkatchenko, A.; Oganov, A. R.; Rohl, A. L.; Tuckerman, M. E.; Kahr, B. *Chem. Sci.* **2017**, *8*, 4926–4940.

(4) Brandenburg, J. G.; Grimme, S. *J. Phys. Chem. Lett.* **2014**, *5*, 1785–1789.

(5) Řezáč, J.; Riley, K. E.; Hobza, P. *J. Chem. Theory Comput.* **2011**, *7*, 2427.

(6) Brauer, B.; Kesharwani, M. K.; Kozuch, S.; Martin, J. M. L. *J. Chem. Theory Comput.* **2016**, *18*, 20905–20925.